SUPPLEMENTARY DATA

SUPPLEMENTARY RESULTS

Anti-LCRMP-1 and -CRMP-1 antibody characterizations

We used a synthetic peptide derived from the unique N-terminus of LCRMP-1 to generate a polyclonal antibody against LCRMP-1. We designated this antibody C2, and characterized it for specificity. Immunoblotting revealed that the C2 antibody bound to the LCRMP-1 protein, but not to the 66-kDa CRMP-1 protein or any other CRMP family protein (Supplementary Figure 1A, middle panel). In contrast, our previously reported monoclonal anti-CRMP-1 antibody [#16-2 (6)] recognized both CRMP-1 and LCRMP-1 in immunoblotting experiments (Supplementary Figure 1A, bottom panel). Because CRMP-1 and LCRMP-1 differ in their molecular sizes (66 kDa versus 80 kDa), the immunoreactive bands representing these two proteins could be easily differentiated when antibody #16-2 was used for immunoblotting. Another monoclonal anti-CRMP-1 antibody (Y21) (5) recognized CRMP-1 but not LCRMP-1 in immunoblotting experiments (Supplementary Figure 1B). We also used the sequence of mouse TUC-4b to clone human LCRMP-4, and found that C2 binds to LCRMP-1 but not LCRMP-4 (Supplementary Figure 1C).

The addition of 40-fold and 80-fold excess concentrations of full-length LCRMP-1 or CRMP-1 proteins (as competitors) could completely block the specific bindings of antibody C2 to LCRMP-1 or antibody #16-2 to CRMP-1 (Supplementary Figure 1D).

The polyclonal anti-LCRMP-1 antibody, C2, and the monoclonal anti-CRMP-1 antibody, Y21, could also be used for immunohistochemical staining. We found that preabsorption of these antibodies with full-length His-LCRMP-1 or -CRMP-1 proteins could immunohistochemically block the LCRMP-1- or CRMP-1-specific staining in lung cancer

tumor specimens (Supplementary Figure 1E, panels I and II). Furthermore, in a tumor tissue specimen from a patient that was known to be positive for CRMP-1 expression (as determined using Y21) and negative for LCRMP-1 (using C2), the CRMP-1 signal could be completely out-competed by the addition of full-length His-CRMP-1 (panel III, third column) but not His-LCRMP-1 (panel III, forth column).

For immunofluorescence staining, we generated another polyclonal antibody (C1) using a bacterially expressed protein corresponding to the unique N-terminus of LCRMP-1. To characterize the specificity of the C1 antibody, we used full-length His-LCRMP-1 protein to preabsorb this antibody, and confirmed that the specific fluorescence signal could be completely blocked (Supplementary Figure 1F).

SUPPLEMENTARY METHODS

Cell Culture Conditions

Cells were grown in culture medium containing 10% FBS and 2 mM L-glutamine (all from Invitrogen, Eugene, OR) at 37°C in a humidified atmosphere of 5% CO_2-95% air. Adherent cells were detached from the culture dishes using a 0.1% trypsin solution containing 0.05% EDTA in phosphate-buffered saline (PBS, 0.01 M sodium phosphate, 0.14 M NaCl, pH 7.4) (Sigma, St. Louis, MO). For the functional assays, cells were transferred to trypsin-free 0.02% EDTA in PBS to avoid damaging the cell surface antigens. Prior to each experiment, all cell phenotypes were verified as being consistent with the American Type Culture Collection's description or the appearance of the original derived cell line (for CL cells).

Plasmid Constructs

The cDNAs encoding full-length human LCRMP-1, deletion mutants Δ22, Δ72, Δ105, and Δ127, point mutants P28AQ30A and R29AK31A and full -length CRMP-1 were amplified from the CL (human lung adenocarcinoma) cell line by polymerase chain reaction (PCR). The amplified cDNAs were subcloned into the pEGFP-C1 or C3 (Clontech, Mountain View, CA) vectors for generation of N-terminal GFP-tagged recombinant proteins. Full-length LCRMP-1 and CRMP-1 proteins tagged at their N-termini with Flag, Myc, HA or red fluorescent protein (RFP) were generated by inserting the appropriate cDNAs into the pCMV-Tag 2A, pCMV-Tag 3A, pcDNA3.1 (Invitrogen, Eugene, OR), or pDsRed2-C1 (Clontech, Mountain View, CA) vectors, respectively. For lentivirus infection, the full-length LCRMP-1 cDNA was inserted into the pTY-EF plasmid (a kind gift from Dr. H.K. Sytwu at

the Graduate Institute of Medical Sciences, National Defense Medical Center, Taiwan). For generation of polyclonal antibodies, a cDNA fragment encoding the unique N-terminal fragment of LCRMP-1 was PCR amplified and subcloned into pRSET-C (Invitrogen, Eugene, OR). For generation of stably transfected LCRMP-1-silenced clones, 21-oligonucleotide siRNA duplexes targeting LCRMP-1 were inserted into pSilencer 4.1-CMV neo (Ambion, Austin, TX). Plasmid pcDNA3-Cdc42N17 was kindly provided by Dr. Ruey-Hwa Chen (Institute of Biological Chemistry, Academia Sinica, Taiwan).

Antibodies

Monoclonal anti-Flag, -5His, and –β-actin antibodies were purchased from Sigma (St. Louis, MO). Polyclonal anti-human N-WASP, -pan-WAVE, -WAVE-1, -WASP, and -p34 antibodies were purchased from Santa Cruz Biotechnology, Inc. (Santa Cruz, CA). The anti-Myc monoclonal antibody was a kind gift from Dr. S.R. Roffler (Institute of Biomedical Sciences, Academic Sinica, Taiwan). The monoclonal anti-human CRMP-1 antibody was produced in our laboratory as previously described (5). Using the unique N-terminus of LCRMP-1, we generated specific polyclonal anti-LCRMP-1 antibodies for the immunoblotting, immunohistochemistry, and immunofluorescence assays. The specificities of these antibodies were characterized using the appropriate positive and negative controls [e.g., preimmune serum, and primary antibody preabsorbed with immunization antigens].

Bacterial Protein Expression

The LCRMP-1 N-terminus (amino acids 1-127) was cloned into the pRSECT-C

plasmid (Invitrogen, Eugene, OR) and transformed into BL21DE3-competent *E. coli* cells (Stratagene, La Jolla, CA) to produce *E. coli* containing the recombinant LCRMP-1 N-terminal expression vector. The day before protein induction, 50 mL of Luria broth (LB) medium containing 50μg/mL ampicillin was placed in a 250-mL flask and inoculated with a single colony of *E. coli* containing the pRSECT-C LCRMP-1 plasmid, and the culture was grown at 37°C overnight. This overnight culture was then mixed with 500 mL of LB medium containing 50 μg/mL ampicillin, and incubated in a 2-liter flask at 37°C with shaking for 1.5 h, until the cells reach the mid-log growth phase (A_{600} = 0.5-0.8). LCRMP-1 protein expression was induced by the addition of isopropyl-β-d-thiogalactopyranoside (IPTG) to a final concentration of 200 μM, followed by incubation at 37°C with aeration for 3 h. The cells were then harvested by centrifugation at 5000 g for 15 min at 4°C and subjected to do protein purification.

Overexpression of LCRMP-1 and CRMP-1 in Lung Cancer Cells, and Selection of Stable Clones

Plasmids pCMV-Tag 2A-CRMP-1, pCMV-Tag 2A-LCRMP-1, pCMV-Tag 3A-CRMP-1, and pSilencer-LCRMP-1 (3.5 μg each) were transfected into 70% confluent CL_{1-0} or CL_{1-5} cells using 20 U of Lipofectamine reagent (Invitrogen, Eugene, OR) in a total volume of 1 mL of Opti-MEM (Invitrogen, Eugene, OR), as described previously (51). Other CL_{1-0} or CL_{1-5} cells were transfected with insert-free pCMV-Tag 2A, pCMV-Tag 3A, and pSilencer-scramble siRNA as negative controls. Gentamycin (G418; Merk, Darmstadt, Germany) was added at a concentration of 450 μg/mL to select single or pooled stable transfectants; the selection medium was changed every 3 days for a 3-week period.

Gentamycin-resistant clones were isolated and allowed to proliferate for further characterization. Integration of the transfected plasmid DNA into the chromosomal DNA was confirmed by immunoblotting analysis. For transient transfections, 70% confluent cultures of CL_{1-0}, CL_{1-5}, or CL_{1-5}-F4 cells were transfected with pEGFP-LCRMP-1, N-terminal deletion constructs of pEGFP-LCRMP-1, pcDNA3-Cdc42N17, pCMV-Tag 2A-CRMP-1, pCMV-Tag 2A-LCRMP-1, or pDsRed-CRMP-1, using the methods described above. Thirty hours later, cells were fixed with 3.7% paraformaldehyde in PBS (pH 7.2), stained with anti-Flag (for pCMV-Taq 2A) or anti-Myc (for pcDNA3) antibodies, and examined using a Zeiss Axiophot epifluorescence microscope equipped with an MRC-1000 laser-scanning confocal imaging system (Bio-Rad Laboratories, Hercules, CA). Lysates from selected clones stably expressing LCRMP-1 were examined by immunoblotting analysis.

SiRNA Preparation and Transfection

Twenty-one-oligonucleotide siRNA duplexes were designed and synthesized to target human LCRMP-1 and WAVE-1. A scrambled sequence was used as a negative control (these sequences are shown in Supplementary Table 3). CL_{1-5}-F4, A549, or CL_{1-0} cells overexpressing LCRMP-1 were seeded to six-well culture plates at 1.5×10^5 cells per well, and incubated at 37°C overnight. siRNA transfection was carried out using Oligofectamine (Qiagen, Hilden, Germany) at 37°C for 24 h. The cells were then detached with 0.1% trypsin containing 0.05% EDTA in PBS, and reseeded to a fresh six-well culture plate. The transfected cells were cultured overnight in RPMI containing 10% FBS, silenced again as described above (double silencing), and then cultured for another 72 h prior to

use in experiments.

Lentiviral Infection

For LCRMP-1 overexpression, the pTY-EF-LCRMP-1 and pTY-EF plasmids were used. For short hairpin RNA-mediated knockdown, LacZ and WAVE-1 shRNA-containing lentiviral vectors were obtained from the National RNAi Core Facility (Academia Sinica, Taiwan). The utilized lentiviruses were generated by cotransfection of HEK293T cells with the appropriate lentiviral vector and a packing DNA mix, using Lipofectamine 2000 (Invitrogen, Eugene, OR). Cells were infected at three different Multiplicities of Infection (MOIs) in polybrene (8 μg/mL)-containing medium. Twenty-four hours after infection, the cells were treated with puromycin (final concentration 0.75 μg/mL) and puromycin-resistant clones were selected and pooled.

***In Vivo* Experimental Lung Metastatic Nodule Examination**

Briefly, the lungs were removed, weighed, and fixed in 10% formalin, and the numbers of lung tumor cell colonies were counted under a dissecting microscope. Embedded tissues were sliced into 4-μm sections, and the sections were stained with hematoxylin-eosin for histological analysis. The number of mice (n=10 per group) used for the experiments was based on the goal of having 98% power to detect a two-fold between-group difference in nodule number at $P < 0.05$.

F-actin and G-actin Staining

Stable transfectants ($CL_{1\text{-}0}$/vector, $CL_{1\text{-}0}$/LCRMP-1-overexpressing or

CL_{1-0}/LCRMP-1 point mutant cells) grown on coverslips at 37°C were washed three times in PBS, fixed for 10 min in 3.7% cold paraformaldehyde (Merk, Darmstadt, Germany) in PBS, and permeabilized for 10 min with 0.1% Triton X-100 in PBS. Nonspecific binding was blocked by incubation for 15 min with 3% BSA in PBS. After a 5-min wash with PBS, the cells were incubated for 30 min with 5 U/mL of rhodamine-conjugated phalloidin and FITC-conjugated DNase I (Molecular Probes, Eugene, OR). Additional PBS washes were performed, and the coverslips were mounted on slides using mounting medium (50% glycerol in PBS). The cells were examined and photographed using a Zeiss Axiophot epifluorescence microscope equipped with an MRC-1000 laser scanning confocal imaging system (Bio-Rad Laboratories, Hercules, CA). Independent experiments were performed at least twice, and 100 cells per clone were assessed during each experiment.

Immunoblotting Analysis of F-actin and G-actin

Stable transfectants (CL_{1-0}/vector, CL_{1-0}/LCRMP-1, or CL_{1-0}/LCRMP-1 point mutant cells) were rinsed with PBS at 25°C, scraped from the tissue culture dishes, and homogenized using 26 1/2 G syringes in 200 μL of lysis and F-actin stabilization buffer (50 mM piperazine-N,N′-bis (2-ethanesulfonic acid), 50 mM NaCl, 5 mM $MgCl_2$, 5 mM EGTA, 5% glycerol, 0.1% Nonidet P-40, 0.1% Triton X-100, 0.1% Tween 20, and 0.1% β-mercaptoethanol, pH 6.9; Sigma, St. Louis, MO) at 30°C. The F-actin was then separated from the G-actin by centrifugation at 100,000 × g for 60 min at 37°C. The pellets were resuspended in 200 μL of ice-cold distilled water containing 1 μM cytochalasin D (Sigma, St. Louis, MO) and then incubated on ice for 1 h (for depolymerization of the F-actin). The dissociated F-actin was centrifuged at 14,000 × g for 10 min at 4°C. The

F-actin and G-actin preparations were then subjected to immunoblotting using a monoclonal anti-β-actin antibody (1:20000), and F-actin protein expression was examined relative to constant G-actin expression. Three independent experiments were performed.

Characterization of LCRMP-1-induced Filopodia Dynamics by Non-interferometric Wide-field Optical Profilometric (NIWOP) Super-resolution Bright-field Optical Microscopy

CL_{1-0}/vector (2A10) and CL_{1-0}/LCRMP-1 (1003 and 1015) cells were placed in 35-mm plastic dishes and cultured at 37°C in a humidified atmosphere of 5% CO_2-95% air. Eight cells from each group were randomly selected and observed without further treatment. Dynamic NIWOP pictures were obtained every 5 min, and each cell was observed for 25 min. To evaluate the effects of LCRMP-1 on the dynamics of filopodia formation, we counted all filopodia belonging to each selected cell every 5 min, and calculated the 25-min averages from eight randomly selected LCRMP-1-overexpressing cells (1003 and 1015) and vector controls (2A10).

SUPPLEMENTARY TABLES

Supplementary Table 1. CRMP-1 and LCRMP-1 expression in relation to clinical parameters and pathological characteristics*

Parameter	No. of patients	CRMP-1 ≤ 50% (%)	CRMP-1 > 50% (%)	*P*	LCRMP-1 ≤ 50% (%)	LCRMP-1 > 50% (%)	*P*
Number of patients	142	41 (28.9)	101 (71.1)		102 (71.8)	40 (28.2)	
Sex							
Male	64	20 (31.3)	44 (68.8)		47 (73.4)	17 (26.6)	
Female	78	21 (26.9)	57 (73.1)	0.571	55 (70.5)	23 (29.5)	0.700
Histological type†							
Squamous cell carcinoma	14	5 (35.7)	9 (64.3)		12 (85.7)	2 (14.3)	
Adenocarcinoma	123	35 (28.5)	88 (71.5)	0.571	86 (69.9)	37 (30.1)	0.215
Tumor size, cm							
≤ 3	68	16 (23.5)	52 (76.5)		45 (66.2)	23 (33.8)	
> 3	74	25 (33.8)	49 (66.2)	0.178	57 (77.0)	17 (23.0)	0.151
Vascular invasion							
Negative	117	27 (23.1)	90 (76.9)		83 (70.9)	34 (29.1)	
Positive	25	14 (56.0)	11 (44.0)	0.001	19 (76.0)	6 (24.0)	0.610
Lymph node metastasis							
Negative	110	24 (21.8)	86 (78.2)		84 (76.4)	26 (23.6)	
Positive	32	17 (53.1)	15 (46.9)	0.001	18 (56.3)	14 (43.7)	0.026
Extranodal extension							
Negative	122	29 (23.8)	93 (76.2)		92 (75.4)	30 (24.6)	
Positive	20	12 (60.0)	8 (40.0)	0.001	10 (50.0)	10 (50.0)	0.019
Tumor stage							
Stage I	107	23 (21.5)	84 (78.5)		82 (76.6)	25 (23.4)	
Stage II	17	7 (41.2)	10 (58.8)		13 (76.5)	4 (23.5)	
Stage III–IV	18	11 (61.1)	7 (38.9)	0.001	7 (38.9)	11 (61.1)	0.004
CRMP-1 expression, %							
≤ 50	41	–	–		23 (56.1)	18 (43.9)	
> 50	101	–	–	–	79 (78.2)	22 (21.8)	0.008
LCRMP-1 expression, %							
≤ 50	102	23 (22.6)	79 (77.4)		–	–	
> 50	40	18 (45.0)	22 (55.0)	0.008	–	–	–

* *P* values were calculated using a two-sided chi-squared test. Abbreviations: CRMP-1, collapsin response mediator protein-1; LCRMP-1, long-form collapsin response mediator protein-1.

† Adenosquamous carcinomas are not included

Supplementary Table 2. *P* values for the sensitivity analysis of the immunohistochemical staining results

Level of expression, %*	*P* value**	
	CRMP-1	LCRMP-1
20	< 0.001	< 0.001
30	0.0011	< 0.001
40	< 0.001	< 0.001
50	< 0.001	< 0.001
60	< 0.001	< 0.001
70	< 0.001	< 0.001
80	0.0035	0.044

* ”Level of expression” reflects the percentage of cells expressing the protein in question, as detected by immunohistochemical staining.

****** *P* values (two-sided) were calculated using log-rank tests.

Note: The cut-off points for CRMP-1 and LCRMP-1 were examined at 10% intervals from 20% to 80%, and Kaplan-Meier analyses and log-rank tests were performed using the different cut-off values.

Supplementary Table 3. Sequences of the 21-oligonucleotide siRNA duplexes

Target gene*	Sequence	Vendor, location
LCRMP-1	5′-CAgCgAggACACggCCAgCgA-3′	Qiagen, Valencia, CA
WAVE-1	5′-AUAUgAUCCACgUAUgUCUgAggUC-3′	Invitrogen, Eugene, OR
Scrambled	5′-AATTCTCCgAACgTgTCACgT-3′	Qiagen, Valencia, CA

*****Abbreviations, LCRMP-1, long-form collapsin response mediator protein-1; WAVE, WASP family verprolin-homologous protein.

Pan *et. al* Supplementary Figure 1

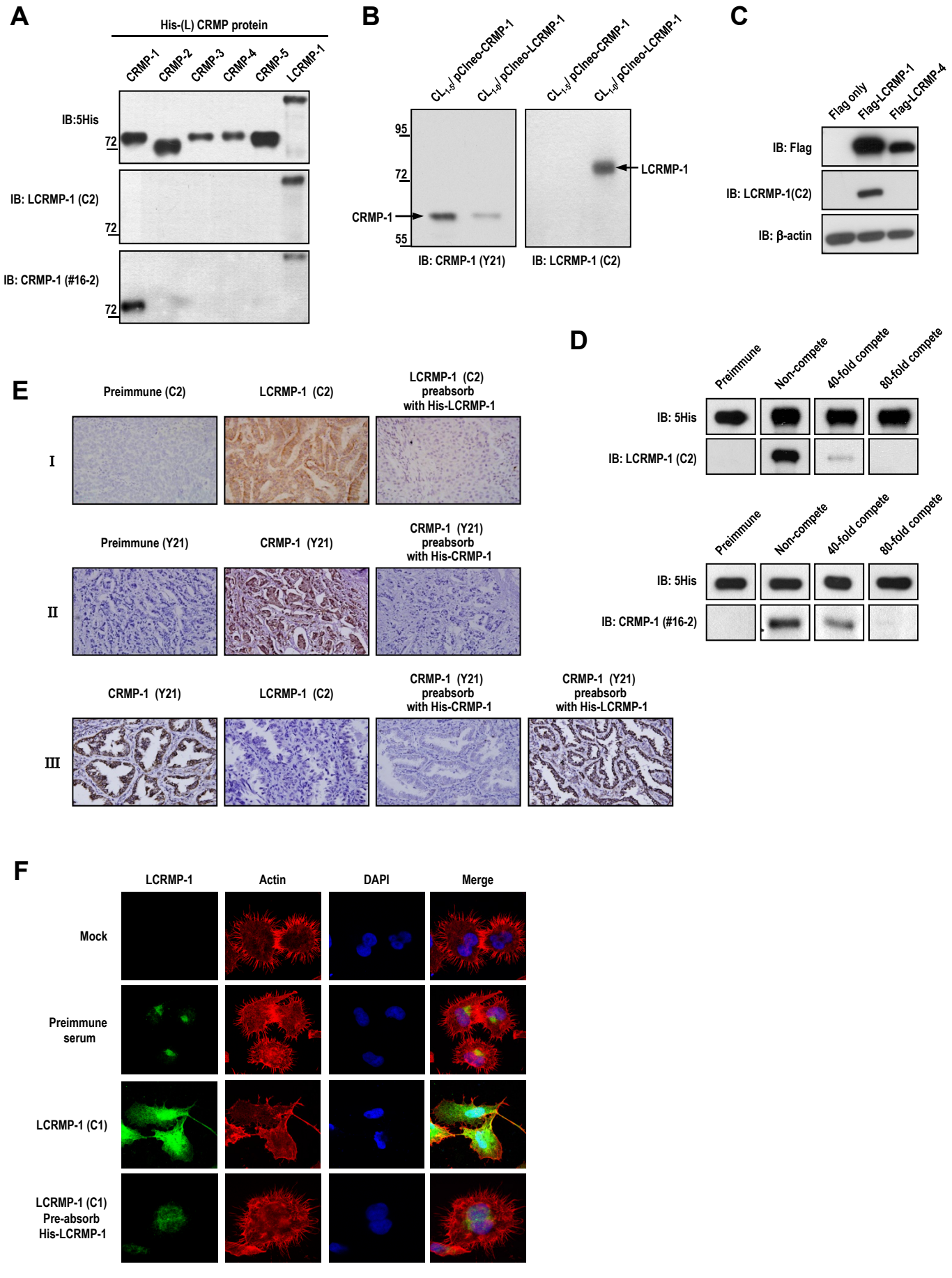

Supplementary Figure 1. Characterization of LCRMP-1 and CRMP-1 antibodies.

(A) Characterizations of anti-LCRMP-1 polyclonal antibody (C2) and anti-CRMP-1 monoclonal antibody (#16-2). Upper panel shows expression level of 5His-tagged (L)CRMP family proteins, as revealed using anti-5His antibody. Middle panel shows LCRMP-1 polyclonal antibody recognizes 5His-tagged LCRMP-1, but not other CRMP family proteins. Bottom panel shows anti-CRMP-1 monoclonal antibody recognizes both 5His-tagged CRMP-1 and LCRMP-1 proteins. **(B)** Characterization of anti-LCRMP-1 polyclonal antibody (C2) and anti-CRMP-1 monoclonal antibody (Y21). Lysates of CL_{1-5}/pCIneo-CRMP-1 and CL_{1-0}/pCIneo-LCRMP-1 were used to examine for presence of CRMP-1 and LCRMP-1 by immunoblotting (IB) with anti-CRMP-1 (Y21, left) and anti-LCRMP-1 (C2, right) antibodies. **(C)** LCRMP-1 antibody (C2) recognizes Flag-LCRMP-1 but not Flag-LCRMP-4. CL_{1-0} cells transfected with pCMV-2A (Flag only), pCMV-2A-LCRMP-1 (Flag-LCRMP-1), or pCMV-2A-LCRMP-4 (Flag-LCRMP-4), and examined presence of Flag-tagged LCRMP-1 and LCRMP-4 by immunoblotting with anti-Flag and anti-LCRMP-1 (C2) antibodies. **(D)** Competition assay of anti-LCRMP-1 polyclonal antibody (C2) and anti-CRMP-1 monoclonal antibody (#16-2). Using 40-fold (lane 3) and 80-fold (lane 4) full length LCRMP-1 protein (upper panel) or full length CRMP-1 (lower panel) as competitors, the specific binding of antibody C2 to LCRMP-1 and antibody #16-2 to CRMP-1 can be completely blocked compared with noncompeted control (lane 2). Upper panel shows the expression pattern of 5His-tagged LCRMP-1 and CRMP-1 proteins, as revealed using anti-5His antibody. **(E)** Characterization of the specificity of anti-LCRMP-1 polyclonal antibody (C2) and anti-CRMP-1 monoclonal antibody (Y21) used in immunohistochemical staining. Tissue specimens were stained with preimmune serum (panel I and II, left), LCRMP-1 polyclonal antibody (C2, panel I, middle), LCRMP-1 polyclonal antibody (C2) preabsorbed with full length His-LCRMP-1 protein (panel I, right), CRMP-1 monoclonal antibody (Y21, panel II, middle), and CRMP-1 monoclonal antibody (Y21) preabsorbed with full length His-CRMP-1 protein (panel II, right). Specific LCRMP-1 or CRMP-1 staining can be blocked immunohistochemically after preabsorbing the antibody with full length His-LCRMP-1 or His-CRMP-1 proteins. A patient's tissue specimen positive for CRMP-1 (Y21) and negative for LCRMP-1 (C2) can be completely competed by full length His-CRMP-1 (panel III, third column) but not by His-LCRMP-1 (panel III, forth column). **(F)** Characterization of specificity of anti-LCRMP-1 polyclonal antibody (C1) used in immunofluorescence staining. CL_{1-5} cells were used as the characterization materials (row 1). LCRMP-1 polyclonal antibody (C1) produces specific fluorescence signals (row 3) compared with preimmune serum control (row 2). LCRMP-1 staining signals are completely blocked by tpolyclonal antibody (C1) preabsorbed with full length His-LCRMP-1 proteins (row 4).

Pan *et. al* Supplementary Figure 2

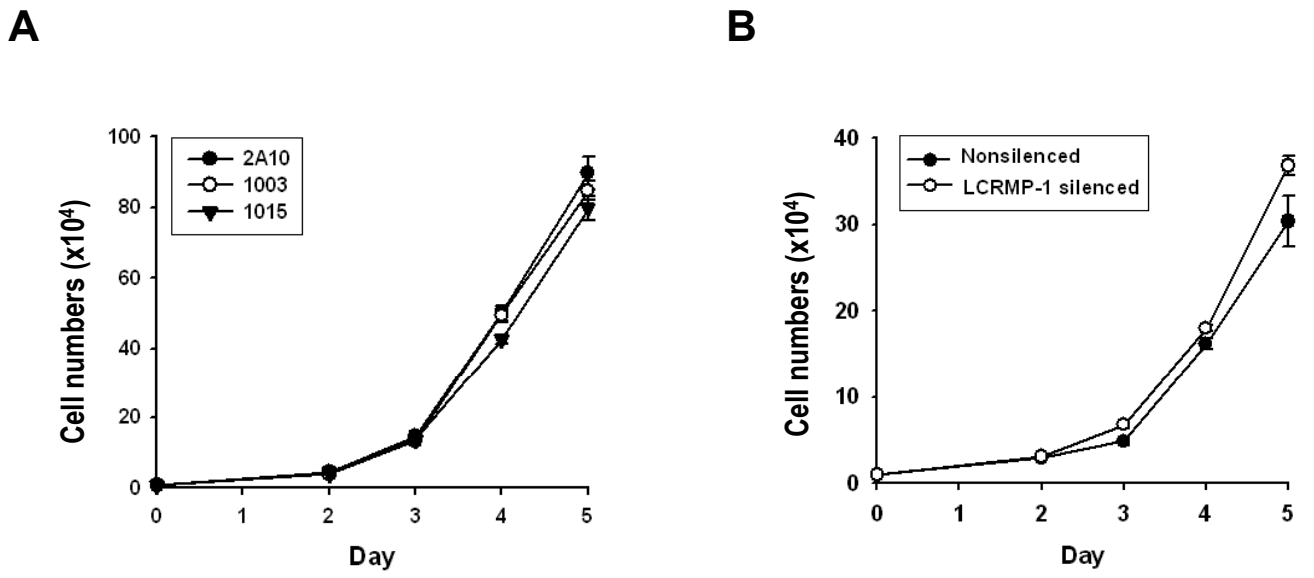

Supplementary Figure 2. LCRMP-1 protein expression does not affect characteristic of cell growth *in vitro*

(A) CL_{1-0} cells constitutively expressing Flag-tagged LCRMP-1 (1003 and 1015) exhibited similar proliferation rate compared with vector control cells (2A10). Data are presented as mean±SEM and *P* values were calculated by two-sided Student's t-test (n=3 experiments). **(B)** CL_{1-5} cells transfected with si-LCRMP-1 (LCRMP-1 silenced) had similar proliferation rate compared with cells transfected with si-scramble (nonsilenced). Error bars indicate mean±SEM and *P* values were calculated by two-sided Student's t-test.

Pan *et. al* Supplementary Figure 3

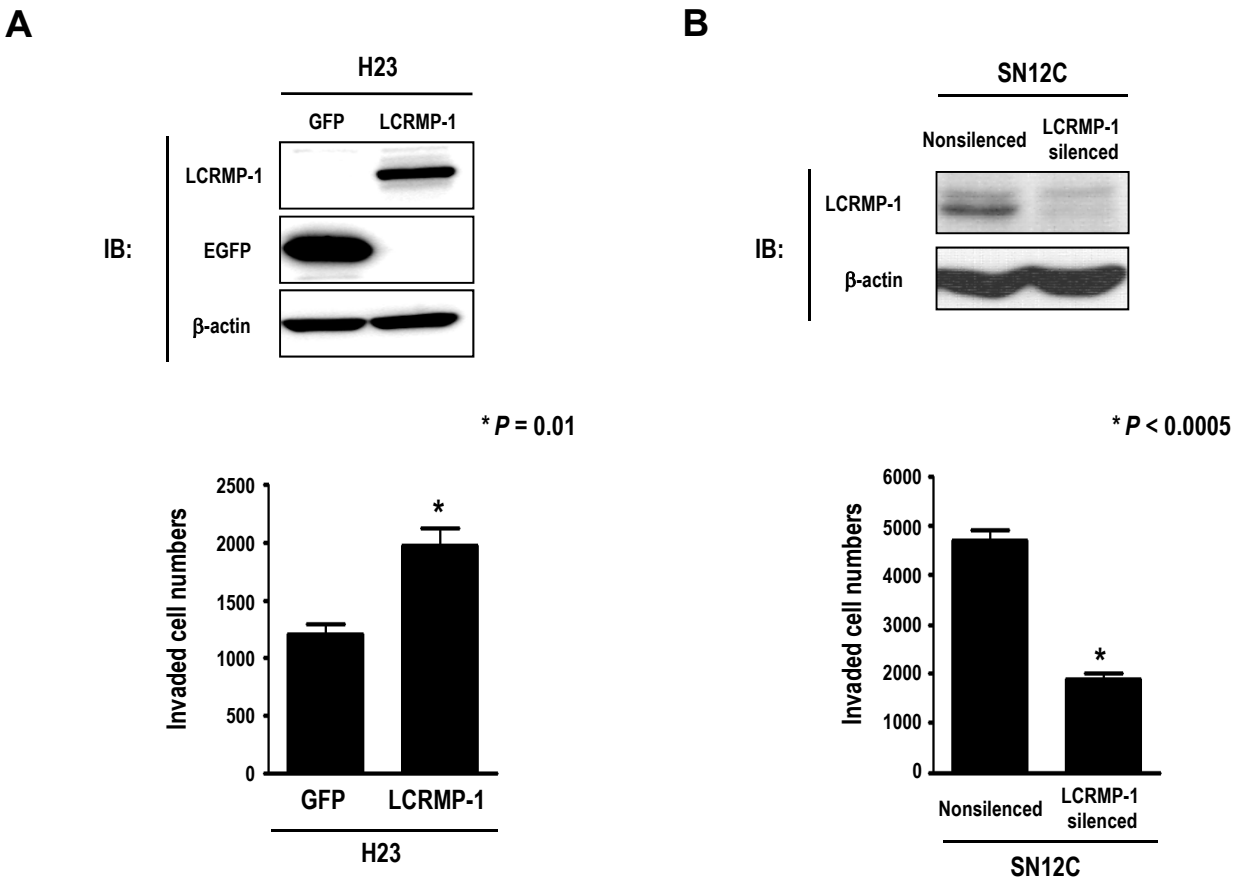

Supplementary Figure 3. LCRMP-1 expression and *in vitro* invasion ability in NCI-60 cell lines, H23 and SN12C

(A) Overexpression LCRMP-1 in H23 cells, which expresses CRMP-1 but not LCRMP-1, promotes cancer cell invasion. Number of invading cells was compared between GFP control and LCRMP-1-expressing clones by an *in vitro* modified Boyden chamber invasion assay. Error bars indicate mean±SEM and *P* values were calculated by two-sided Student's t-test. **(B)** Silenced of LCRMP-1 protein expression in SN12C, which expresses LCRMP-1 but not CRMP-1, decreases invasive abilities. Number of invading cells was compared between nonsilenced control and LCRMP-1-silenced stable clones. Data are presented as mean±SEM and *P* values were calculated by two-sided Student's t-test (n=3 experiments).

Pan *et. al* Supplementary Figure 4

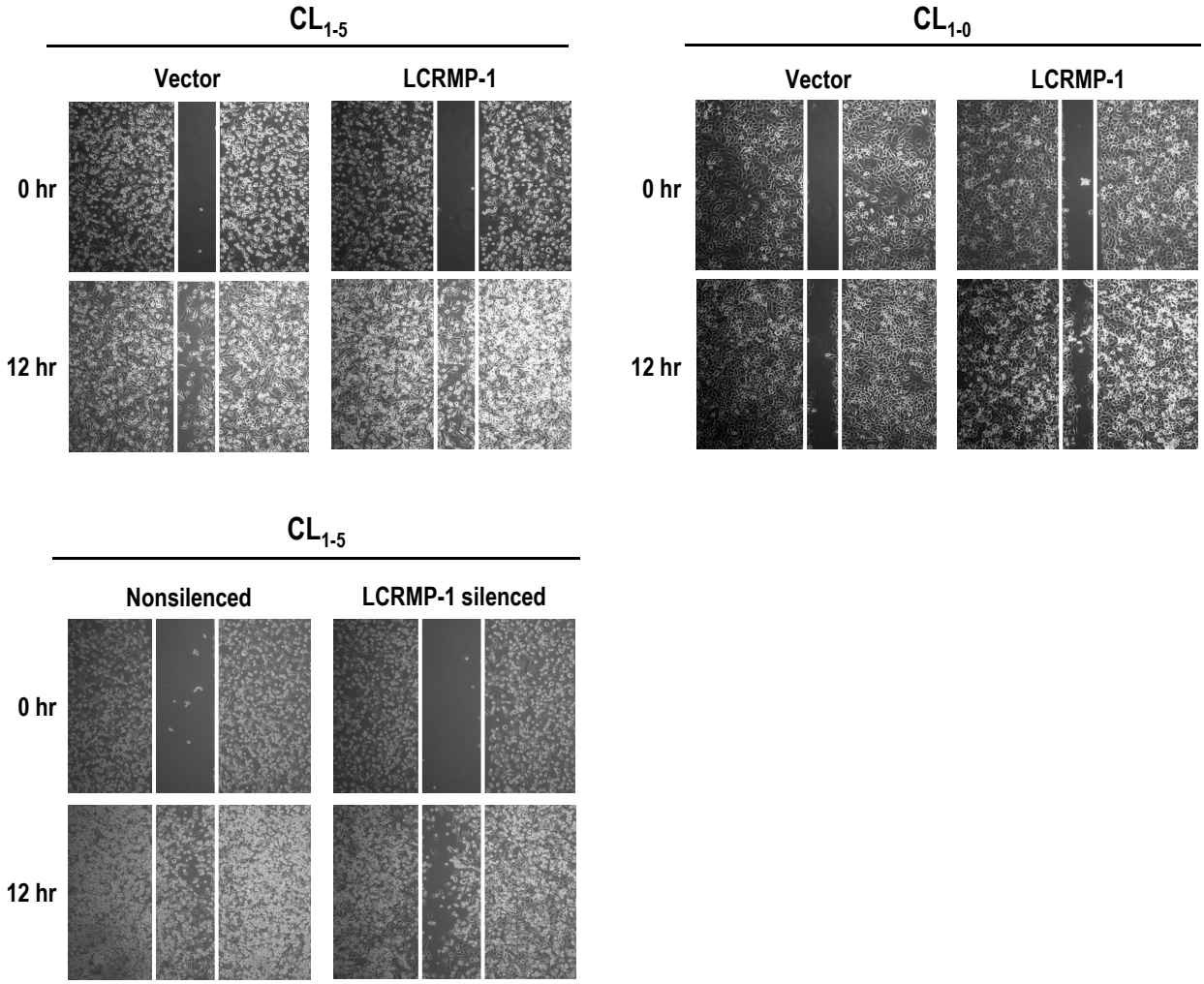

Supplementary Figure 4. Wound images of LCRMP-1 stable expression cells

LCRMP-1 promotes cell migration in CL_{1-0} and CL_{1-5}. Pool stable clones CL_{1-5}/vector control, CL_{1-5}/LCRMP-1 (top left), CL_{1-0}/vector, CL_{1-0}/LCRMP-1 (top right), CL_{1-5}/nonsilenced control, CL_{1-5}/LCRMP-1 silenced (bottom left) were used to examine their migration abilities by wound healing assay. Pictures were taken at 0 and 12 hr after wounding.

Pan *et. al* Supplementary Figure 5

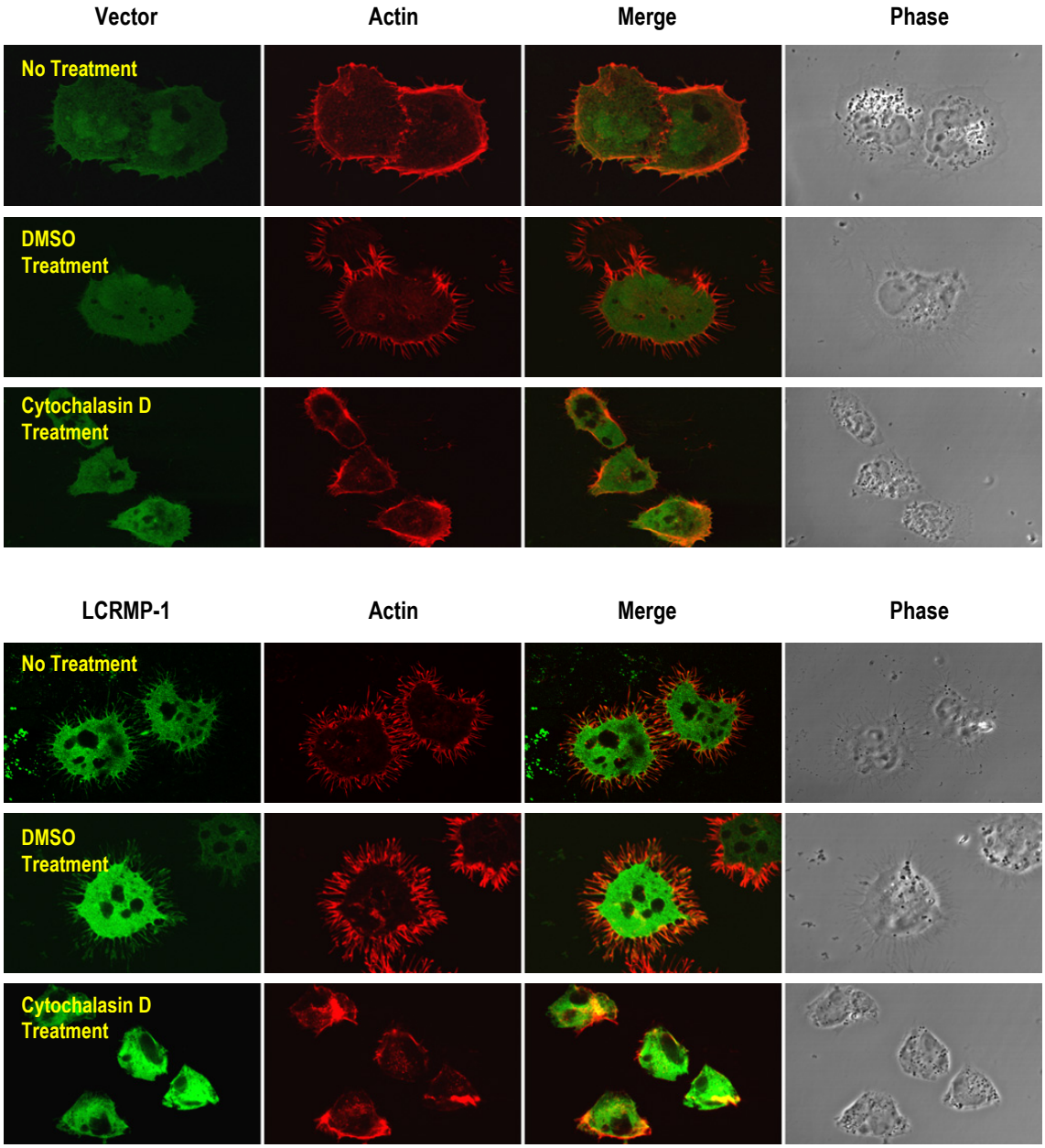

Supplementary Figure 5. Effects of Cytochalasin D on LCRMP-1-induced filopodia in CL_{1-5} cells

CL_{1-5} cells were transfected with pEGFP-LCRMP-1 or pEGFP (green). After 24 hr, cells were treated with DMSO or cytochalasin D for 1 hr, and then stained with rhodamine-conjugated phalloidin (actin, red) and examined for filopodia formation.

Pan *et. al* Supplementary Figure 6

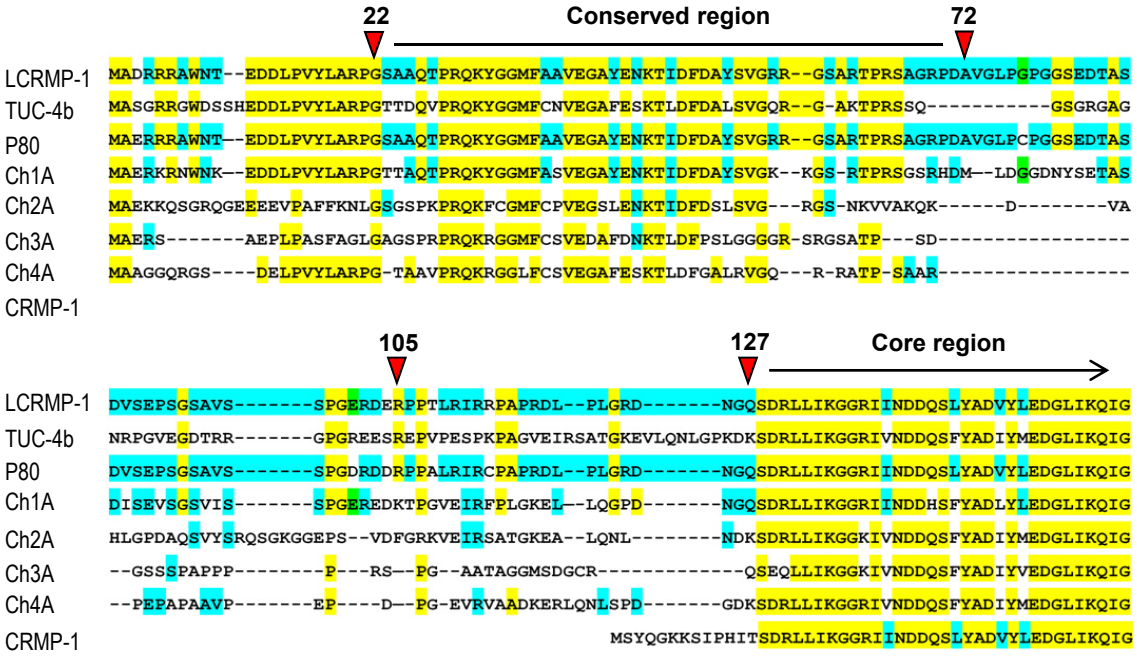

Supplementary Figure 6. Amino acid alignment of N-terminal sequences of human LCRMP-1, CRMP-1, mouse CRMP-A (p80 and TUC-4b), and chicken CRMP-A (Ch1A~4A)

Residues 22–72 are highly conserved among the longer forms (yellow), and the core region is identical to CRMP-1 after residue 127. Sequences in blue are common to individual subtypes of CRMP-1, whereas residues shown in yellow are common to all CRMP family proteins. Numbers 22, 72, 105, and 127 indicate sites of deletions discussed in Figure 2C.

Pan *et. al* Supplementary Figure 7

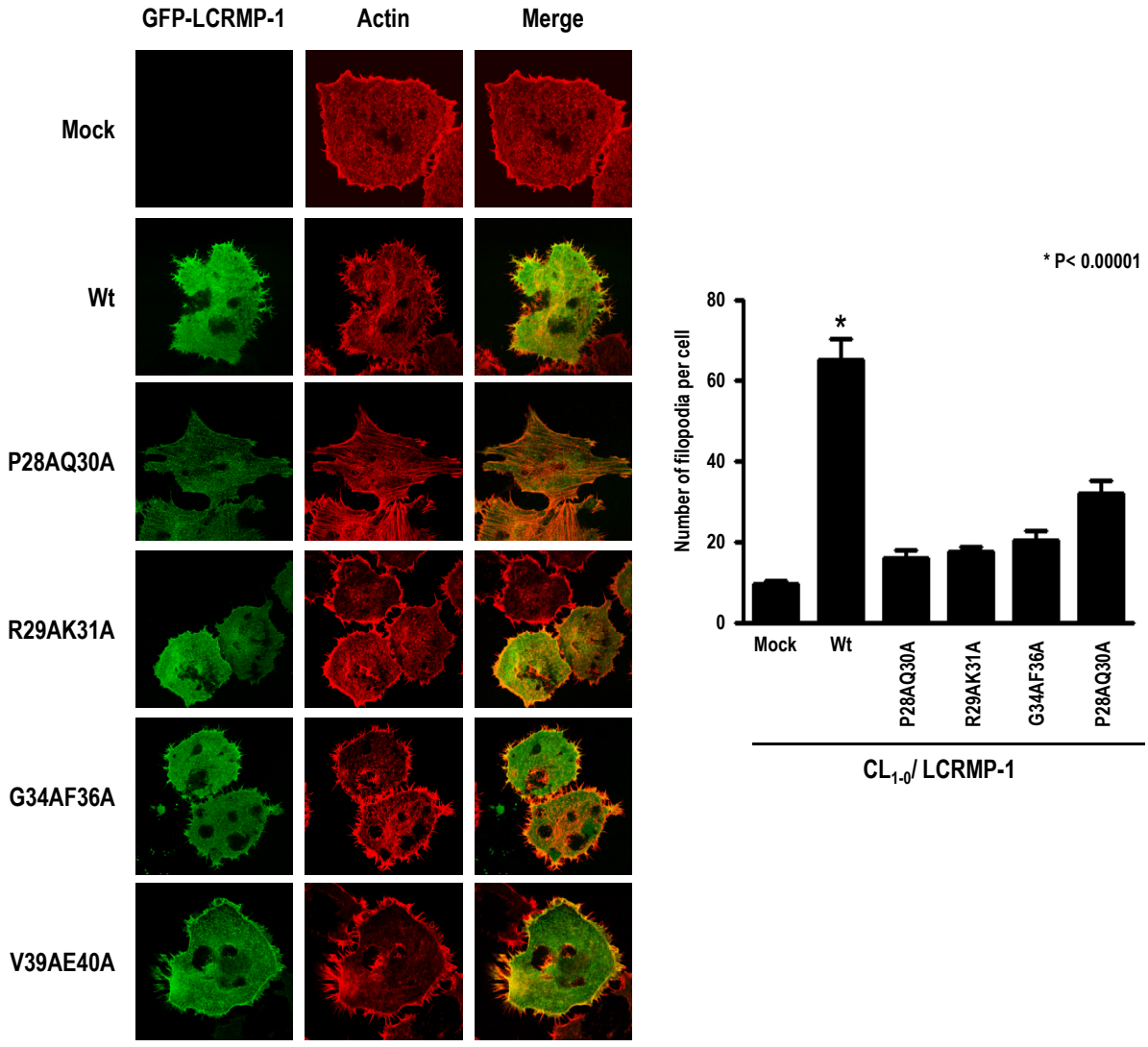

Supplementary Figure 7. Filopodia formation by LCRMP-1 or LCRMP-1 point mutation mutants

$CL_{1\text{-}0}$ cells were transfected with different LCRMP-1 point mutation constructs (Wt, P28AQ30A, R29AK31A, G34AF36A, and V39AE40A) labeled with GFP (green). After 30 hr, the cells were stained with rhodamine-conjugated phalloidin (actin, red) and examined for filopodia formation. Number of filopodia per cell was calculated from 20 cells in each group (n= 3 experiments). Data are presented as mean±SEM and *P* values were calculated by two-sided Student's t-test.

Pan *et. al* Supplementary Figure 8

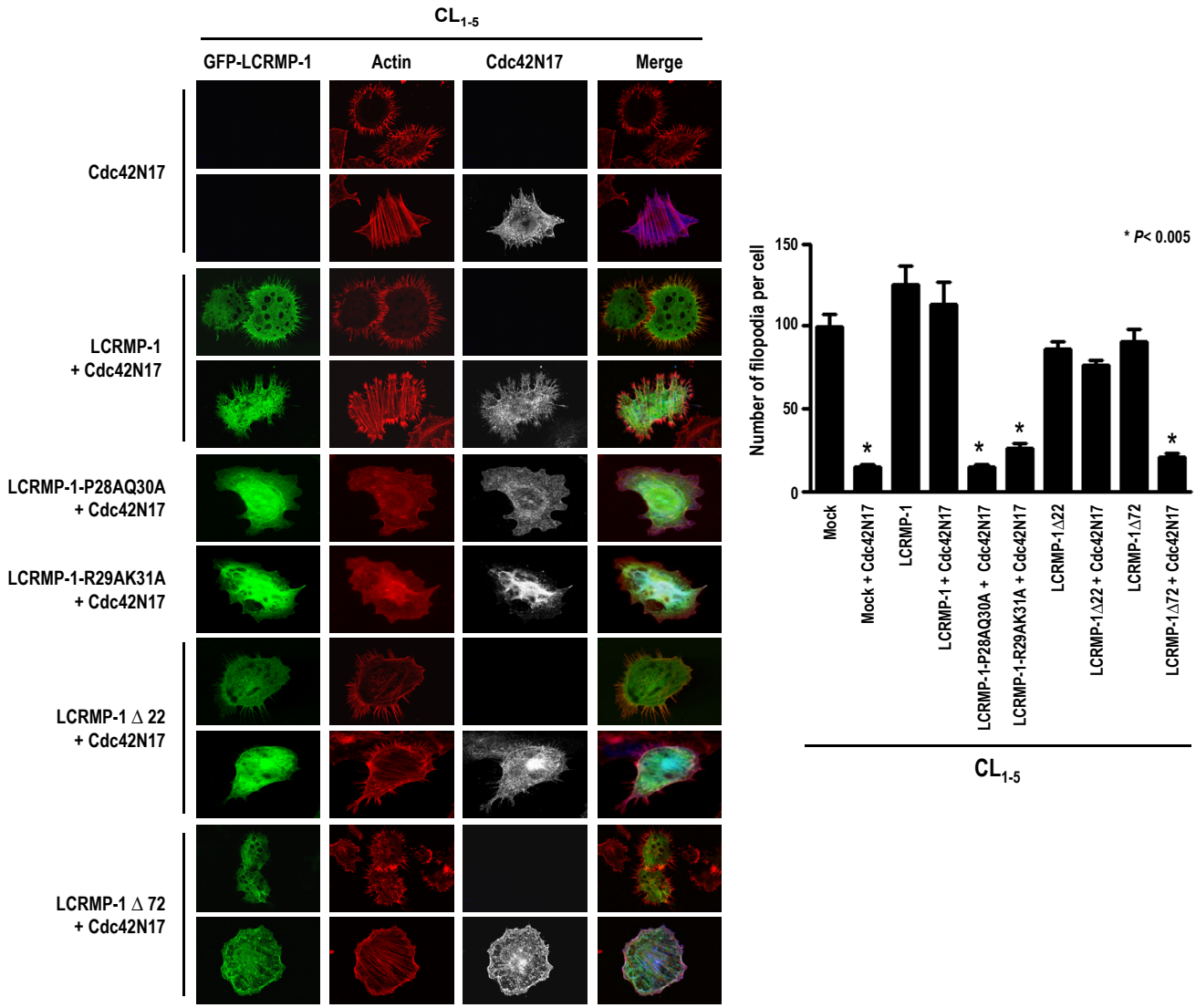

Supplementary Figure 8. Function of LCRMP-1 N-terminus on Cdc42 dominant negative induced filopodia repression

Deletion or mutation in N-terminal residues 22–72 of LCRMP-1 abolishes the effect of LCRMP-1 which is to reverse the dominant negative effect of Cdc42 on filopodia formation. Ability of different LCRMP-1 deletion or mutation constructs to reverse the effect of dominant negative Cdc42 on filopodia formation was examined in highly invasive CL_{1-5} cells. CL_{1-5} cells were cotransfected with various pGFP-LCRMP-1 deletion or mutation constructs that shown in Figure 2C and pcDNA3-Cdc42N17. After 30 hr, cells were fixed and stained with rhodamine-conjugated phalloidin (actin, red) and Cy5-labeled anti-Myc antibody (Cdc42N17, gray) in order to analyze the effect on filopodia formation. Number of filopodia per cell was calculated from 20 cells in each group (n= 3 experiments). Error bars indicate mean±SEM and *P* values were calculated by two-sided Student's t-test.

Pan *et. al* Supplementary Figure 9

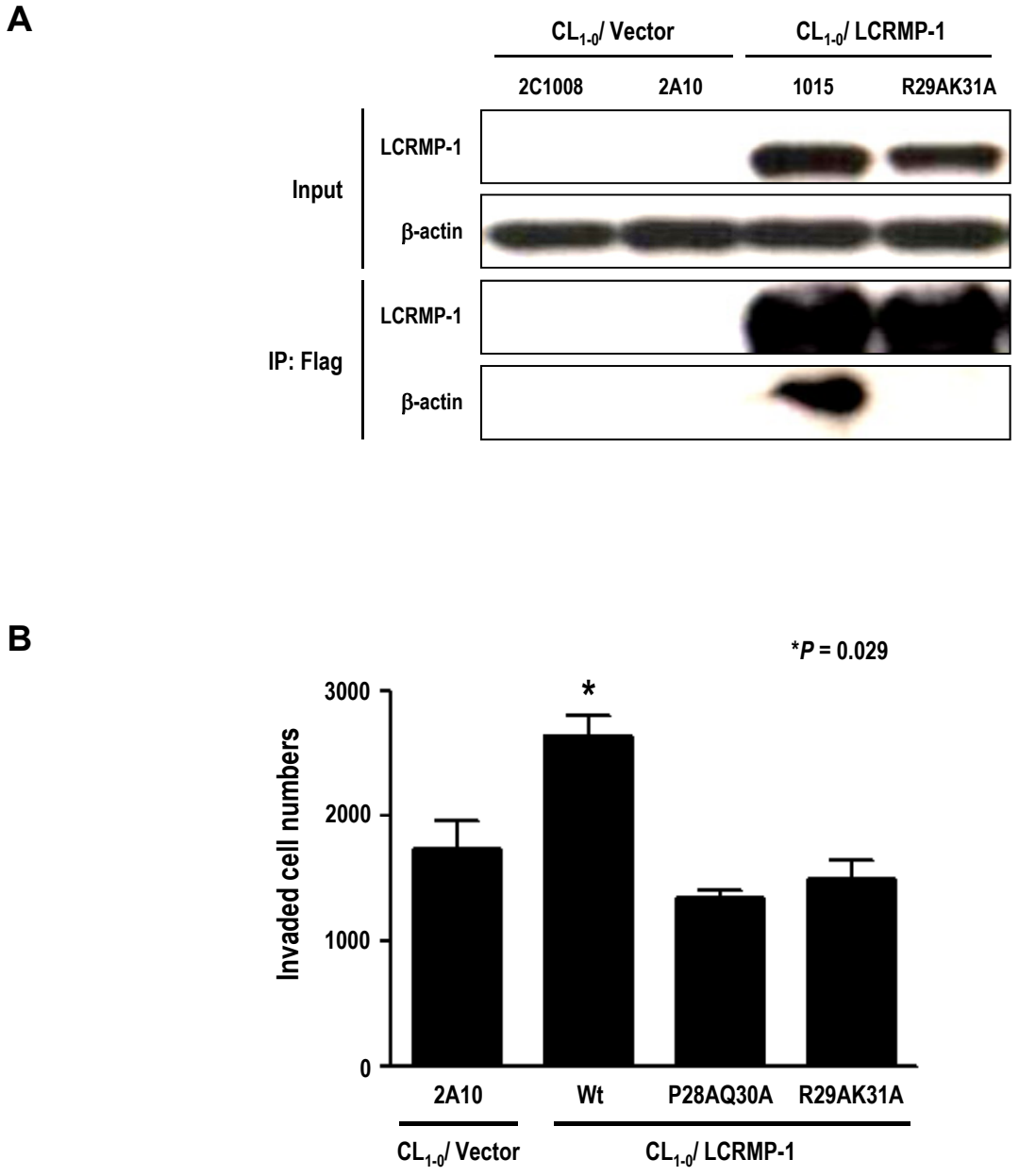

Supplementary Figure 9. Characterization of LCRMP-1 residues 22-72 on actin binding and cell invasiveness

(A) LCRMP-1 can bind to actin, as shown in a comparison of LCRMP-1-overexpressing CL_{1-0} clones (1015) versus vector control (2A10 and 2C1008). Binding ability is abrogated by mutation of residues 22–72 (R29AK31A, n= 2 experiments). **(B)** LCRMP-1, but not LCRMP-1 mutant, expression increases cancer cell invasive ability. Number of invading cells from LCRMP-1-expressing clones (Wt) and LCRMP-1 mutant-expressing clones (P28AQ30A and R29AK31A) were compared with vector control cells (2A10) by an *in vitro* modified Boyden chamber invasion assay (n= 3 experiments). Error bars indicate mean±SEM and *P* values were calculated by two-sided Student's t-test.

Pan *et. al* Supplementary Figure 10

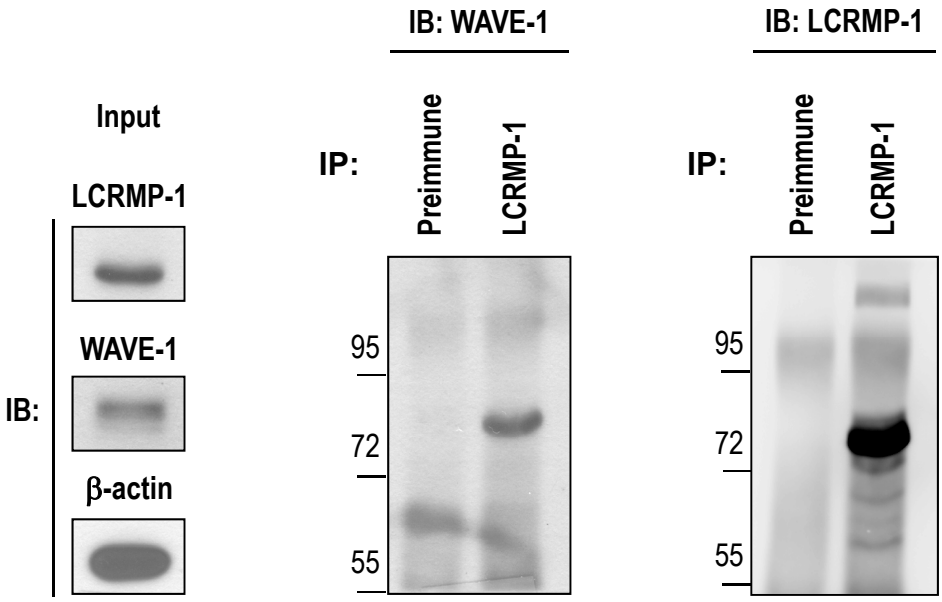

Supplementary Figure 10. **Endogenous LCRMP-1 can interact with WAVE-1 in a NCI-60 cell line, H522**

Total cell lysates (15 mg) from H522 cells were immunoprecipitated (IP) with anti-LCRMP-1 (C2) antibody and binding of WAVE-1 was analyzed by immunoblotting using anti-WAVE-1 or anti-LCRMP-1 (C2) antibodies (n= 2 experiments).

Pan *et. al* Supplementary Figure 11

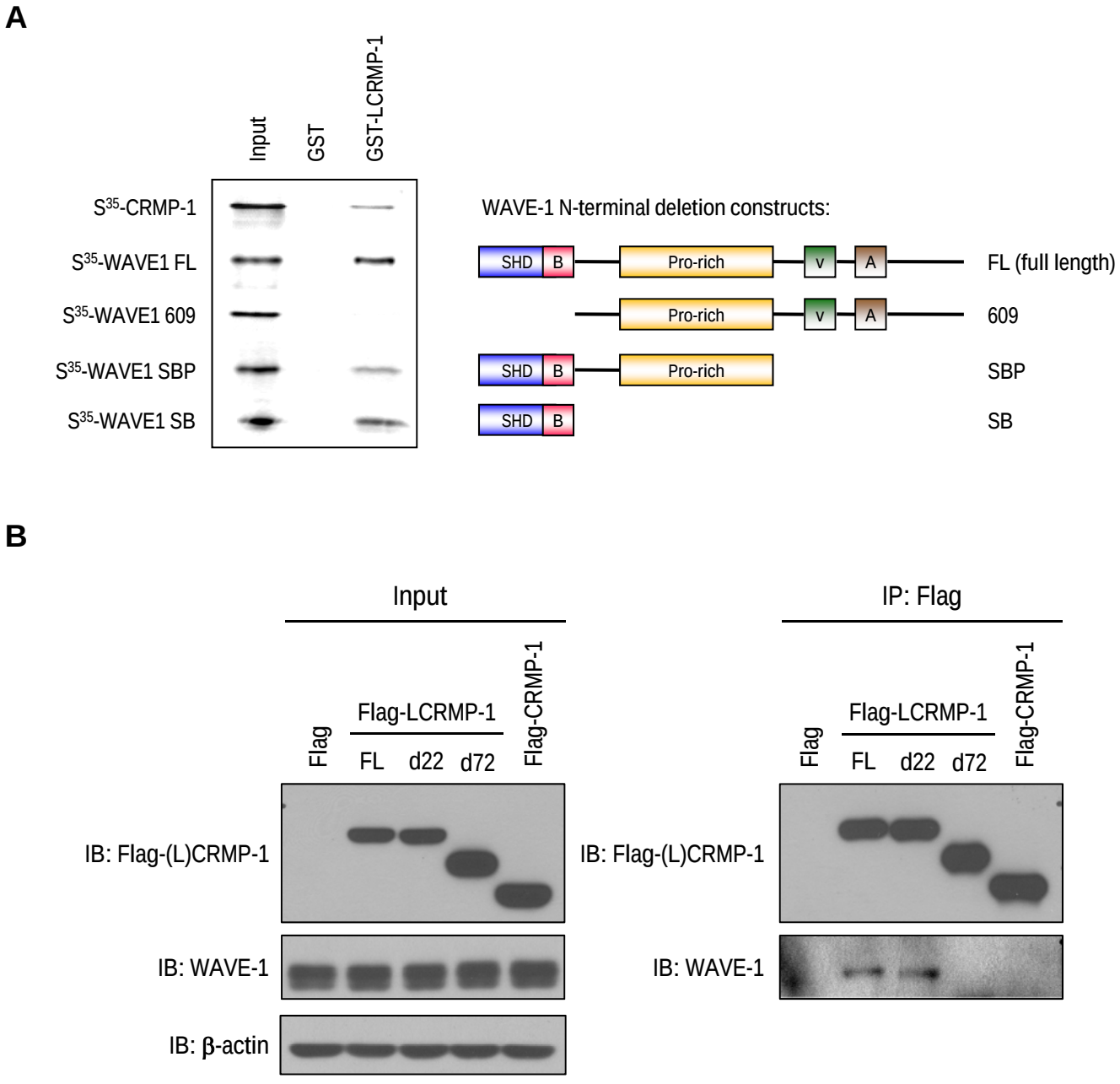

Supplementary Figure 11. Analysis of the binding domain of WAVE-1 with LCRMP-1

(A) Domain mapping of LCRMP-1 and WAVE-1 by *in vitro* transcription/translation and GST pull-down assay. GST and GST-LCRMP-1 were pulled down with S^{35}-labelled WAVE-1 full length (FL) and WAVE-1 deletion constructs (609, SBP and SB), and CRMP-1(served as positive control). **(B)** Lysates of Flag-tagged LCRMP-1, LCRMP-1 deletion mutants or CRMP-1 stable expressing cells were immunoprecipitated (IP) with anti-Flag antibody, and examined binding of WAVE-1 by immunoblotting.

Pan *et. al* Supplementary Figure 12

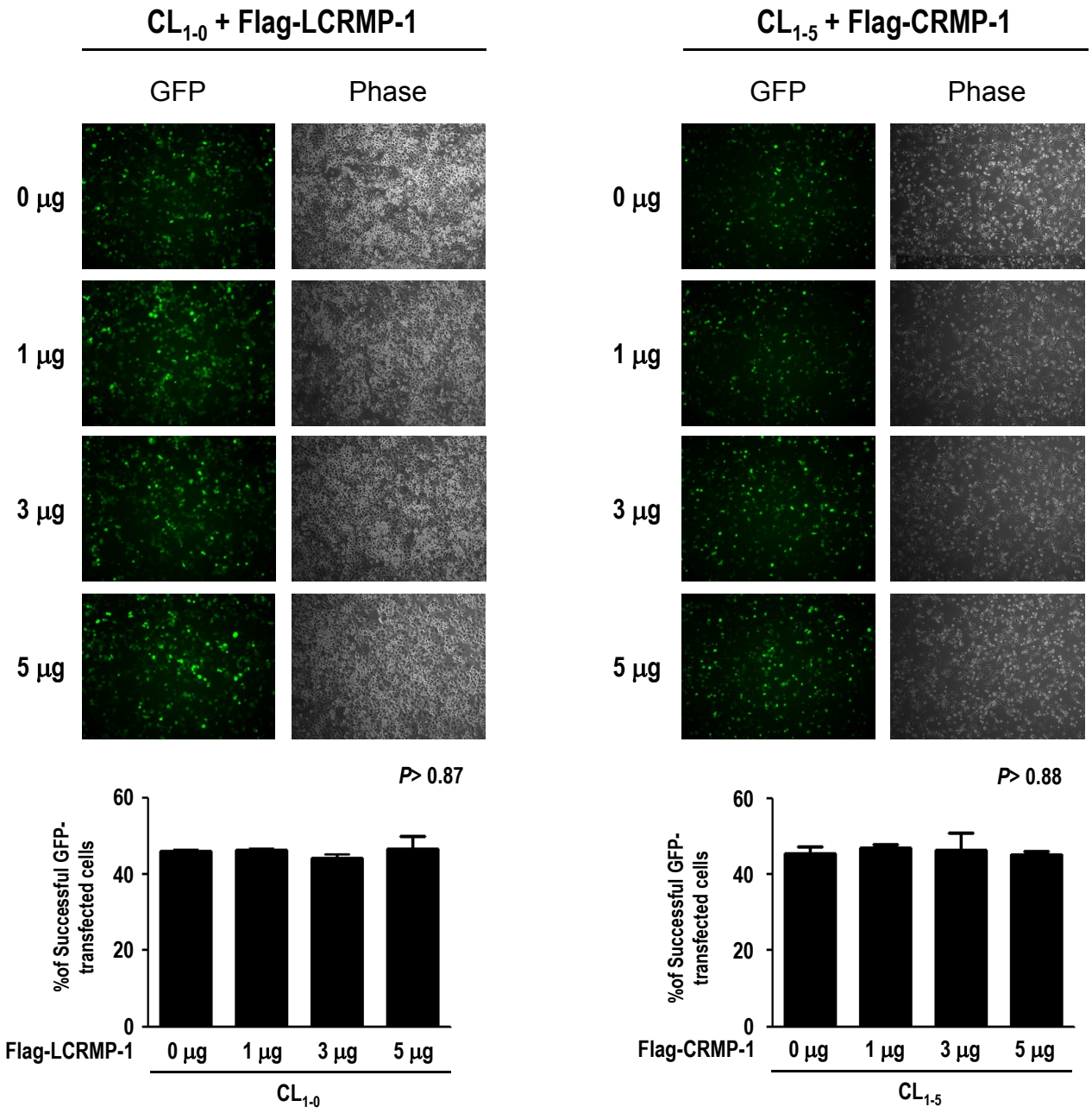

Supplementary Figure 12. Transfection efficiency of experiment in Figure 6A

Left: Less-invasive CL_{1-0} cells, which typically express endogenous CRMP-1 but not LCRMP-1, were transfected with different amounts of pCMV-Tag 2A-LCRMP-1 (Flag-LCRMP-1). Equal amounts of pEGFP plasmids were also co-transfected into the cells as a control of transfection efficiency. Percentage of GFP-transfected cells was quantified from 3 random selected regions. **Right:** An identical experiment was performed using highly invasive CL_{1-5} cells, which endogenously express LCRMP-1 but not CRMP-1, transfected with pCMV-Tag 2A-CRMP-1 (Flag-CRMP-1). Data are presented as mean±SEM and *P* values were calculated by two-sided Student's t-test.

Pan *et. al* Supplementary Figure 13

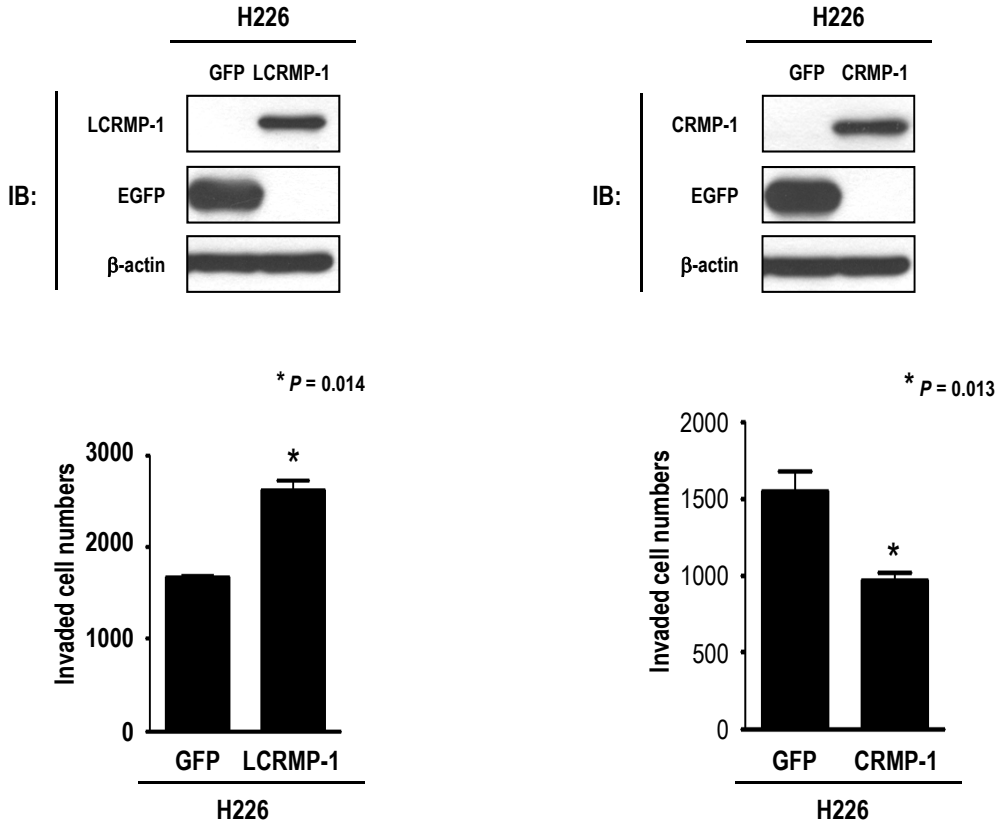

Supplementary Figure 13. LCRMP-1 expression and *in vitro* invasion ability in a NCI-60 cell line, H226

Opposite functions of LCRMP-1 and CRMP-1 on H226 cancer cell invasion. H226 cells express neither LCRMP-1 nor CRMP-1 proteins. The comparison of number of invading cells in an *in vitro* modified Boyden chamber invasion assay between GFP control and LCRMP-1-expressing or CRMP-1-expressing clones are evaluated (n= 3 experiments). Error bars indicate mean±SEM and *P* values were calculated by two-sided Student's t-test.

Pan *et. al* Supplementary Figure 14

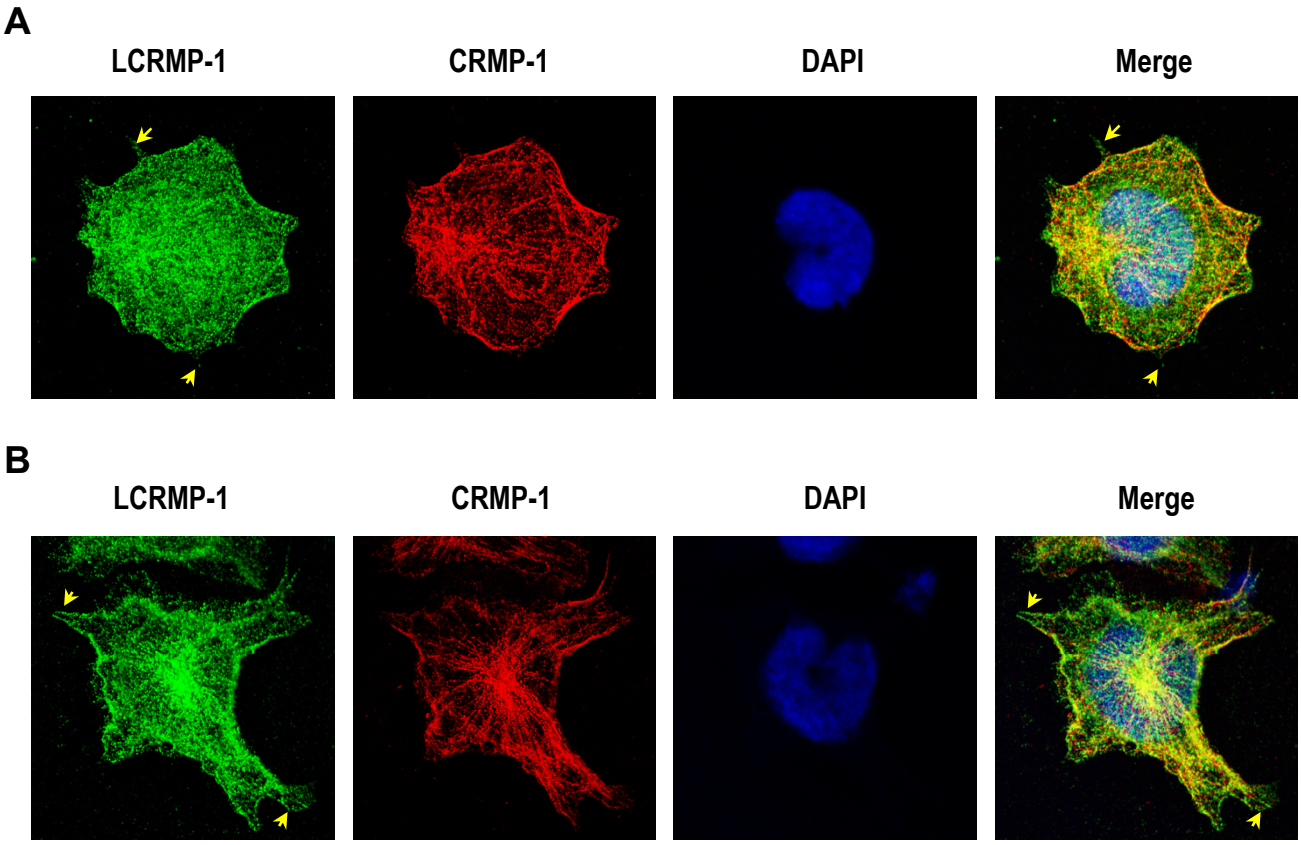

Supplementary Figure 14. Localization of endogenous LCRMP-1 and CRMP-1 in a NCI-60 cell line, H522

H522 cells were fixed with 3.7% cold paraformaldehyde, stained with LCRMP-1 and CRMP-1 specific antibodies, and then with FITC- (green for LCRMP-1) or rhodamine- (red for CRMP-1) conjugated secondary antibodies. A and B are two individual cells.

Pan *et. al* Supplementary Figure 15

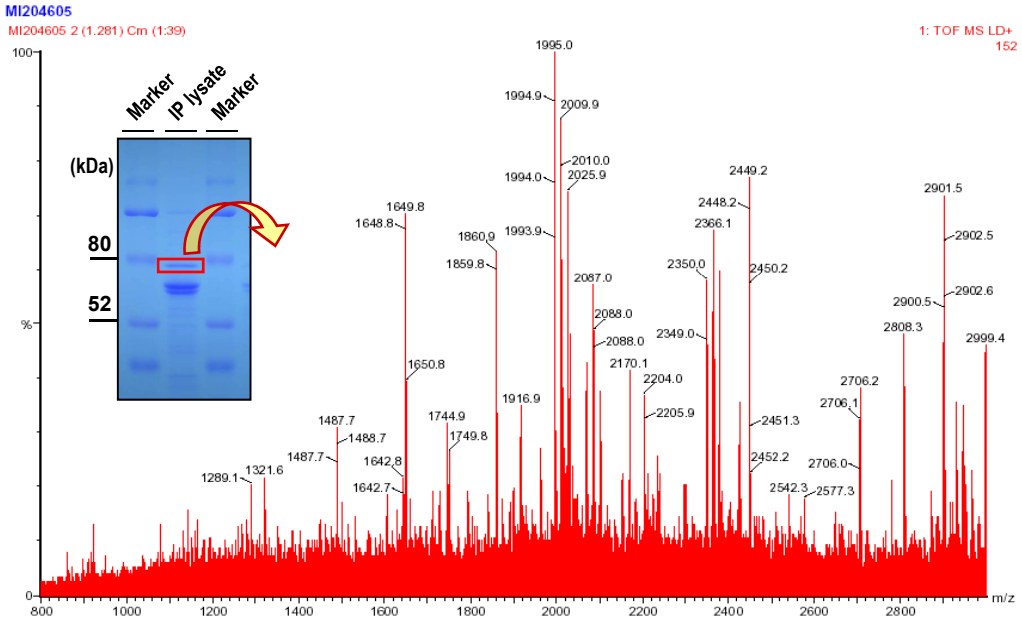

Supplementary Figure 15. Identification of CRMP-1 associated protein, p80 (LCRMP-1) by mass spectrometry

Immunoprecipitation was performed using 30 mg total cell lysates from $CL_{1\text{-}0}$/CRMP-1 overexpression stable cells and 30 μg anti-Flag antibodies. The resulting 80 kDa band was excised, followed by in-gel digestion, and the peptides were characterized by liquid chromatography coupled with tandem mass spectrometry (LC-MS/MS).

Pan *et. al* Supplementary Figure 16

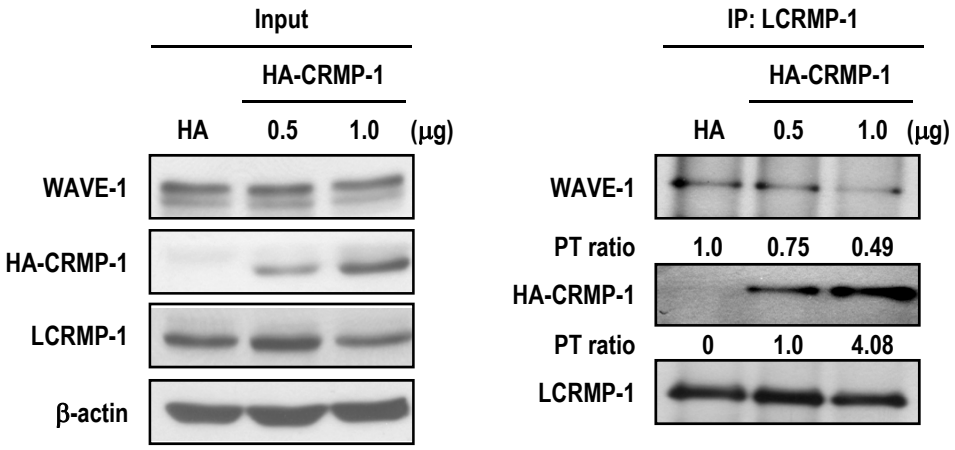

Supplementary Figure 16. CRMP-1 inhibits endogenous binding of LCRMP-1 with WAVE-1

Cell lines constitutively expressing different amounts of HA-CRMP-1 was established by transfecting pcDNA3.1-HA-CRMP-1 into CL_{1-5} cells. Pool colonies were chosen following selection with 450 μg/mL G418. Cell lysates were immunoprecipitated (IP) with anti-LCRMP-1 antibody (C2), and binding of WAVE-1 and HA-CRMP-1 was examined by immunoblotting. In cells expressing high levels of HA-CRMP-1 expression (1.0 μg), binding ability of LCRMP-1 and WAVE-1 was significantly decreased. Similar results were obtained from two independent experiments.

Pan *et. al* Supplementary Figure 17

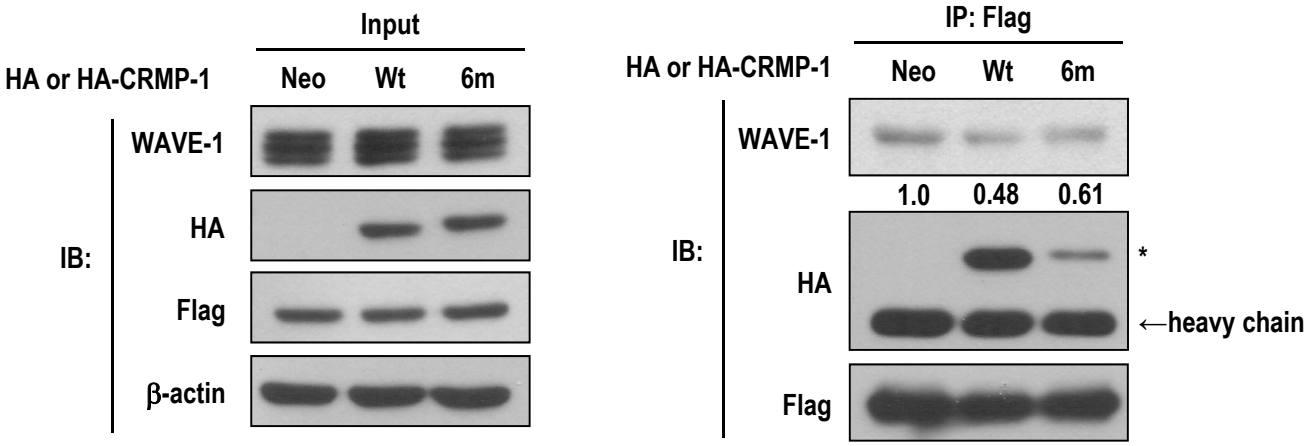

Supplementary Figure 17. CRMP-1 mutant partially reverses CRMP-1's inhibition on binding between LCRMP-1 and WAVE-1.

Lentivirus infection system was used to express CRMP-1 (Wt) and CRMP-1 mutant (6m) in $CL_{1\text{-}0}$/LCRMP-1 cells (1003). Cell lysates were immunoprecipitated (IP) with anti-Flag antibodies, and binding of WAVE-1 and CRMP-1 was examined by immunoblotting (IB). In cells expressing CRMP-1 mutant, binding ability of LCRMP-1 and CRMP-1 was significantly decreased (star, right); and binding ability between LCRMP-1 and WAVE-1 was partial reversed (n= 2 experiments).

Pan *et. al* Supplementary Figure 18

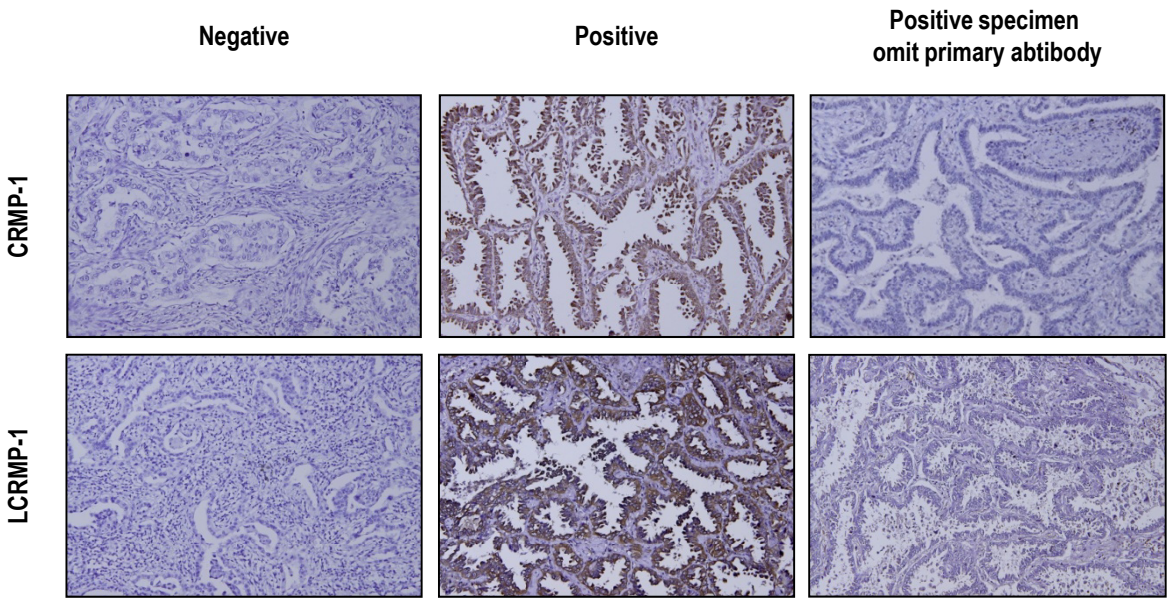

Supplementary Figure 18. Specificity of CRMP-1 and LCRMP-1 antibodies in immunohistochemical staining

Tumor specimens were used for immunohistochemical staining by CRMP-1 (Y21, up) and LCRMP-1 (C2, down) antibodies. CRMP-1 and LCRMP-1 positive staining (middle column) had strong signals in cancer cells when compared with the negative specimens (left column) or those positive specimens but omit the usage of primary antibodies (right column).

Pan *et. al* Supplementary Figure 19

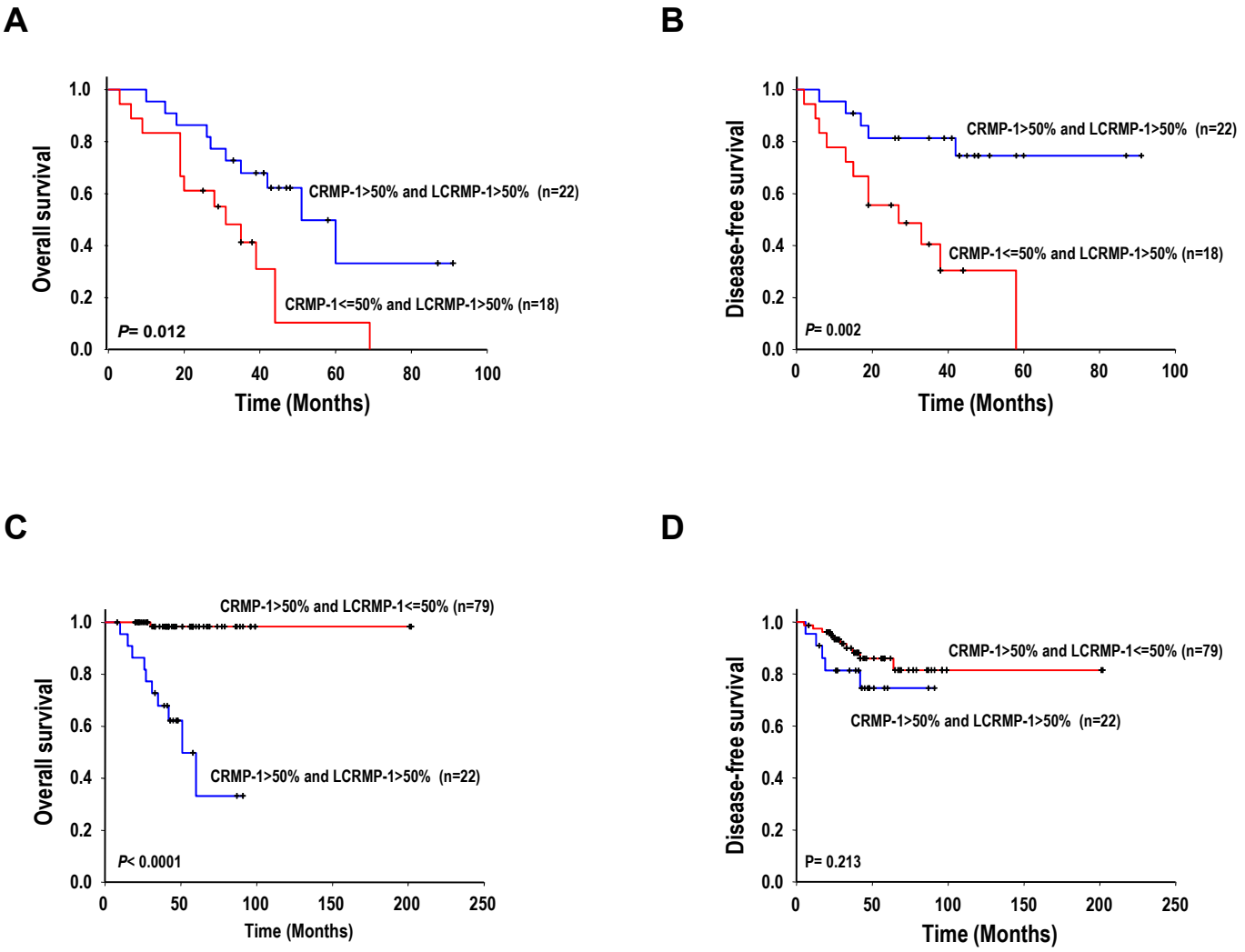

Supplementary Figure 19. Kaplan-Meier survival plots for NSCLC patients grouped by LCRMP-1 and CRMP-1 protein expression levels

Patients were designated as having 'high (L)CRMP-1 expression' if more than 50% of the neoplastic cells in their tumor sections were immunoreactive, and as having 'low (L)CRMP-1 expression' if fewer than 50% were immunoreactive. The results shown reflect Kaplan–Meier estimates of overall survival and disease-free survival of the NSCLC patients according to their expression levels. **(A)** Overall survival of high LCRMP-1 and CRMP-1 expresisons compared with high LCRMP-1 and low CRMP-1 expressions. **(B)** Disease-free survival of high LCRMP-1 and CRMP-1 expresisons compared with high LCRMP-1 and low CRMP-1 expressions. **(C)** Overall survival of high LCRMP-1 and CRMP-1 expresisons compared with high CRMP-1 and low LCRMP-1 expressions. **(D)** Disease-free survival of high LCRMP-1 and CRMP-1 expresisons compared with high CRMP-1 and low LCRMP-1 expressions. *P* values were obtained from two-sided log-rank tests.

Pan *et. al* Supplementary Figure 20

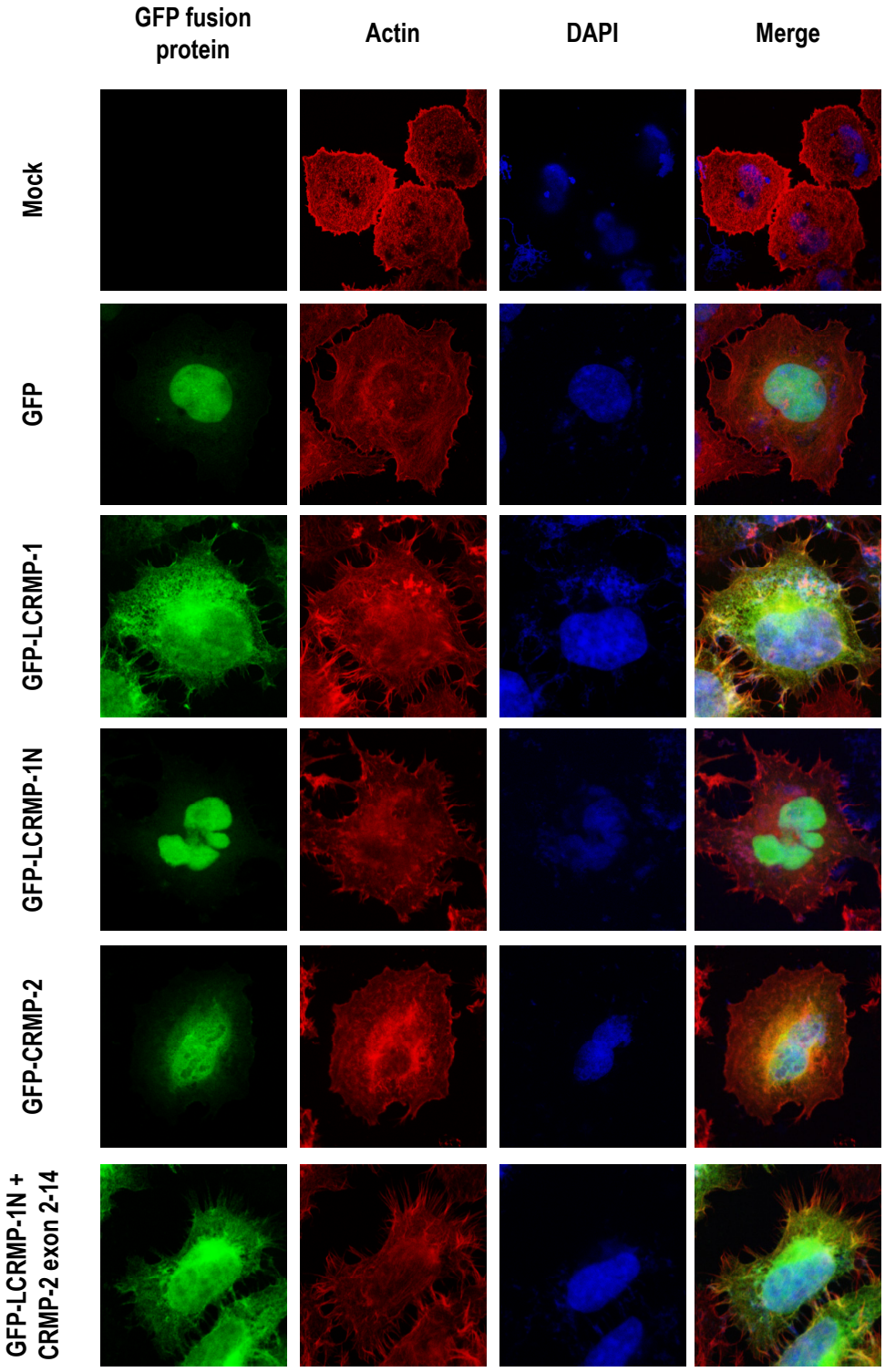

Supplementary Figure 20. LCRMP-1 N-terminus promotes filopodia formation in CL_{1-0} cells

CL_{1-0} cells were transfected with GFP-LCRMP-1, exon-1 of LCRMP-1 (LCRMP-1N), CRMP-2 and LCRMP-1 N fused with CRMP-2 exon 2-14 (green). After 30 hr, cells were stained with rhodamine-conjugated phalloidin (actin, red) and examined for filopodia formation.